

# Tuning of the Fano Effect through a Quantum Dot in an Aharonov-Bohm Interferometer

Kensuke Kobayashi<sup>1</sup>, Hisashi Aikawa<sup>1</sup>, Shingo Katsumoto<sup>1,2</sup>, Yasuhiro Iye<sup>1,2</sup>

<sup>1</sup>*Institute for Solid State Physics, University of Tokyo, 5-1-5, Kashiwanoha, Chiba 277-8581, Japan*

<sup>2</sup>*CREST, Japan Science and Technology Corporation, Mejiro, Tokyo 171-0031, Japan*

(May 21, 2019)

The Fano effect, which arises from an interference between a localized state and the continuum, represents one of the most fundamental aspects of quantum mechanics as observed in many physical systems. We have realized a tunable Fano system in a quantum dot (QD) in an Aharonov-Bohm interferometer, which is the first convincing demonstration of this effect in mesoscopic systems. With the aid of the continuum, the localized state inside the QD acquires itinerancy even in the Coulomb blockade. By tuning the system in several ways, its unique properties on the phase and coherence of electrons have been revealed.

When a discrete energy level is embedded in a continuum energy state and there is coupling between these two states, a resonant state arises around the discrete level. In 1961, Fano proposed the theory [1] that in such a system, a transition from an arbitrary initial state occurs through two interfering configurations — one directly through the continuum and the other through the resonance level — as sketched in Fig. 1A. Such a quantum mechanical interference yields a characteristic asymmetric line shape in the transition probability. This is the Fano effect, a ubiquitous phenomenon observed in a large variety of experiments including neutron scattering [2], atomic photoionization [3], Raman scattering [4], and optical absorption [5]. While a statistically averaged nature of the system containing contributions from numerous sites is observed in these experiments, the Fano effect is essentially a single-impurity problem describing how a localized state embedded in the continuum acquires itinerancy over the system [6]. Therefore, an experiment on a single site would reveal this fundamental process in a more transparent way. While the single-site Fano effect has been reported in the scanning tunneling spectroscopy study of an atom on the surface [7,8] or in transport through a quantum dot (QD) [9], there is little, if any, controllability in either case since the coupling between the discrete level and the continuum is naturally formed.

To realize a well-defined Fano system, we designed an Aharonov-Bohm (AB) ring with a QD embedded in one of its arms (Fig. 1B), similar to those in several previous studies [10–13]. The AB ring is essentially a double-slit interferometer of electrons. In contrast, the QD [14], a small electron droplet isolated from its leads by tunneling barriers, has discrete energy levels arising from the electron confinement and the charging energy  $e^2/C$  that is much larger than the temperature  $k_B T$  ( $e$  is the charge of the electron,  $C$  is the capacitance of the QD,  $k_B$  is the Boltzmann constant, and  $T$  is the temperature). In the Coulomb blockade (CB) regime, the resultant single-particle level in the QD can be controlled electro-statically by the gate voltage ( $V_g$ ), and only when

the level matches the chemical potential of the leads is conductance through the QD allowed by single-electron tunneling. Thus, our “modified” AB interferometer has the continuum energy state in its metallic arm and the discrete energy level in the QD in the other arm. If the coherence of the electron is fully maintained during tunneling through the QD and during propagation through the arm, interference of traversing electrons will occur through two different configurations. Physically, this situation is exactly a realization of the Fano system [15–17].

Figure 1C shows the fabricated Fano system on a two-dimensional electron gas (2DEG) system at an Al-GaAs/GaAs heterostructure. The ring-shaped conductive region was formed by wet-etching the 2DEG. The metallic gates were deposited to control the device. The three in the lower arm were used for defining a QD and the gate in the upper arm is a control gate to switch the transition through the continuum state on and off. Measurements were performed between 30 mK and 800 mK in a dilution refrigerator by a standard lock-in technique in the two-terminal setup with an excitation voltage of 10  $\mu$ V (80 Hz) between the source and the drain.

First, we pinched off the upper arm by applying large negative voltage on the control gate ( $V_C$ ). After tuning the side-gate voltages ( $V_L$  and  $V_R$ ), the QD was defined in the lower arm, as seen in the pronounced peaks in the conductance  $G$  through the QD, as sweeping the center gate  $V_g$  (lower panel of Fig. 2A). This behavior is a typical Coulomb oscillation expected for QDs in the CB regime. The irregularity of the peak positions reflects that of the addition energy and supports the occurrence of transport through each single level inside the QD.

Next, we made the upper arm conductive. Because the control gate and the QD are well separated electro-statically, a clear one-to-one correspondence is observed between the two results in Fig. 2A, ensuring that the discreteness of the energy levels in the QD is maintained. It is noteworthy that the line shapes of the oscillation become very asymmetric and show even dip structures. This is a clear sign of the Fano effect. Indeed, each peak can be well fitted by the Fano line shape [1]  $G(\epsilon)$  of the

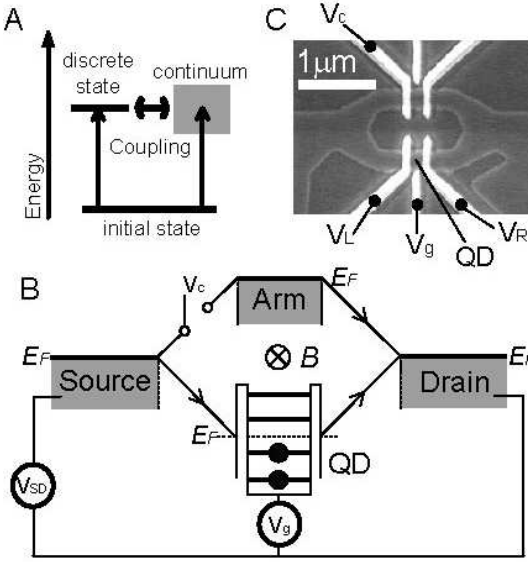


FIG. 1. (A) The principle of the Fano effect. When two interfering paths, one through the discrete state and the other through the continuum, are allowed in transition from an initial state, the Fano effect occurs, resulting in a characteristic spectrum. (B) Schematic representation of our Fano system. An electron injected from the source traverses the ring along two different paths through the arm and the QD and interferes at the drain. The arm, consisting of 2DEG, has a continuum energy spectrum while the QD embedded in the other arm has a single discrete level for the electron to transmit. This corresponds to an artificial single-site Fano system, which is controllable in several ways; the discrete level inside the QD, the coupling between the continuum and the discrete levels, and the phase difference between two paths are controlled by the gate voltage  $V_g$ , the control gate voltage  $V_C$ , and the magnetic field  $B$  penetrating the ring, respectively. In addition, when the temperature increases, the arm and the QD are quantum mechanically decoupled due to loss of coherence. (C) Scanning electron micrograph of the device fabricated by wet-etching the 2DEG in the AlGaAs/GaAs heterostructure (mobility =  $9 \times 10^5 \text{ cm}^2/\text{Vs}$ , sheet carrier density =  $3.8 \times 10^{11} \text{ cm}^{-2}$ , and electron mean free path  $l_e \sim 8 \mu\text{m}$ ). The length of one arm of the ring is  $L \sim 2 \mu\text{m}$ . The Au/Ti metallic gates were deposited on the ring. The three gates ( $V_R$ ,  $V_L$ , and  $V_g$ ) at the lower arm are used for controlling the QD (with area about  $0.15 \times 0.15 \mu\text{m}^2$ ) and the gate at the upper arm is for  $V_C$ . All the measurements were performed between 30 mK and 800 mK using a dilution refrigerator. Noise filters were inserted into every lead at  $T < 1 \text{ K}$  as well as at room temperature.

form

$$G(\epsilon) \propto \frac{(\epsilon + q)^2}{\epsilon^2 + 1}, \quad \epsilon = \frac{V_g - V_0}{\Gamma/2} \quad (1)$$

where  $V_0$  is the energy of the resonance position,  $\Gamma$  is the width of the resonance. The real parameter  $q$  is the ratio of the matrix elements linking the initial state to the

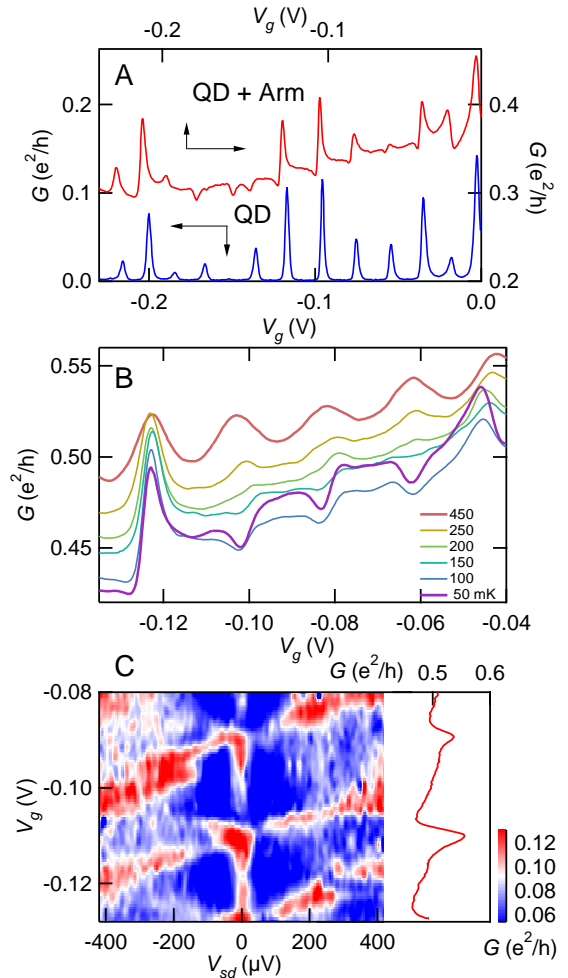


FIG. 2. (A) Typical Coulomb oscillation at  $V_C = -0.12 \text{ V}$  with the arm pinched off, and asymmetric Coulomb oscillation at  $V_C = -0.086 \text{ V}$  with the arm transmissible. The latter shows a clear Fano effect. Both of them were obtained at  $T = 30 \text{ mK}$  and  $B = 0.91 \text{ T}$ . (B) The Fano effect measured at several temperatures at  $B = 0.93 \text{ T}$ . It gradually disappears as the temperature increases. (C) Differential conductance obtained as a function of  $V_g$  at  $T = 30 \text{ mK}$  and  $B = 0.92 \text{ T}$ . The corresponding Fano line shape is also shown in the right panel. The zero-bias conductance peak exists in the CB region with a Coulomb diamond superimposed. Incoherent contribution from the differential conductance of the upper arm, which shows slight non-Ohmic behavior at finite  $V_{sd}$ , has been subtracted from the data.

discrete and continuum parts of the final state. The line shape analysis for several resonance levels gives  $|q| = 0.2 - 7$  with  $\Gamma \sim 3 \text{ meV}$ . The observed  $|q|$  values, which are a measure of the degree of coupling between the discrete state and the continuum, are correlated with the values of the conductance of the original Coulomb peak. The Fano effect was found to occur within several specific magnetic field ( $B$ ) ranges such as around  $B \sim 0.3, 0.9$ , and  $1.2 \text{ T}$ . A similar role of specific magnetic field is reported in the study of the Kondo effect in a QD [12]. Presumably, a

particular magnetic field might favor coherent transport through the QD.

The dip structure with  $|q| < 1$  indicates a strong destructive interference. This implies that the electron passing the QD retains sufficient coherency to interfere with the one passing the arm. While several systems similar to ours have been studied already [10–13], the arm without a QD has been acceptably treated as a “reference” arm since the coherence was limited to only a fraction of the transmission through the QD. In contrast, here, in spite of the significant charging effect inside and around the QD, the transport through the QD occurs coherently enough for the Fano effect to show up over the wide range of the parameters ( $V_g$ ,  $V_C$ , and  $B$ ). As a result, the arm itself functions as an essential part, making our device a quantum mechanically hybridized system.

When the temperature increased, decoherence increased and the asymmetric Fano line shapes at the low temperature gradually evolved into an ordinary Lorentzian line shape corresponding to  $|q| \rightarrow \infty$  (Fig 2B). Due to the loss of coherence over the interferometer at  $T \geq 450$  mK, the system is simply a classical parallel circuit of the QD and the arm, being no longer in the Fano state.

To investigate the non-equilibrium Fano effect, we measured the differential conductance at the lowest temperature as a function of both source-drain bias ( $V_{sd}$ ) and  $V_g$  (Fig. 2C). Superimposed on the Coulomb diamond, the resonating conductance peak of the width  $\sim 70$   $\mu$ eV (colored white and red) stretches along the line of  $V_{sd} = 0$  V. The appearance of the zero-bias conductance peak even in the CB region indicates that the transmission through the QD is now allowed due to the aid of the continuum in the opposite arm. Such delocalization of the electron in the CB region is highly analogous with that observed in the QD in the Kondo regime [18–20], although the mechanism is different. Delocalization in the Kondo dot occurs through resonating spin singlet-pair formation, while resonance due to the configuration interaction between the discrete state and the continuum is the cause in the Fano regime [6].

In our system, the discrete level and the continuum are spatially separated, allowing us to control Fano interference via the magnetic field piercing the ring (Fig. 3A). The line shape changes periodically with the AB period of  $\sim 3.8$  mT, which agrees with that expected from the ring dimension. The oscillation amplitude at the conductance maximum is of the same order as the net peak height, again ensuring that the transmission through the QD occurs coherently. As  $B$  is swept, an asymmetric line shape with negative  $q$  continuously changes to a symmetric one and then to an asymmetric one with positive  $q$ ; the sign of interference can be controlled by the AB effect. Usually, the Fano effect is characterized by an asymmetric line shape, while a perfect symmetric line shape is obtained at a specific magnetic field here. Since

the magnetic field mainly affects the phase difference between the two paths through the resonant state and the continuum, the above-mentioned behavior will be most likely explained systematically by introducing a complex number  $q$  whose argument is a function of  $B$ , though an expression of such  $q$  applicable to our case is not known at present. In the original work by Fano [1] and most of the subsequent studies based on his theory, the asymmetric parameter  $q$  has been implicitly treated as a real number, while this is valid only when the system has the time-reversal symmetry and thus the relevant matrix elements can be taken as real. Our experiment indicates that when this condition is broken, for example, by applying the magnetic field,  $q$  should be a complex number, which has not been explicitly recognized.

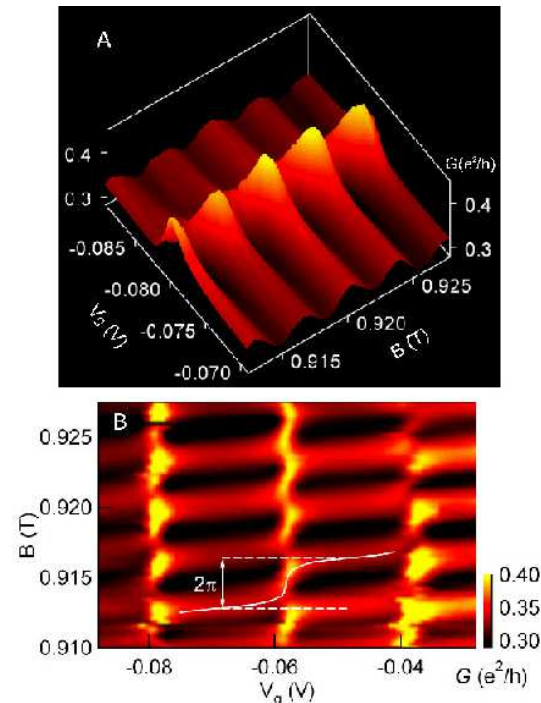


FIG. 3. (A) The conductance of one Fano peak as a function of  $V_g$  and  $B$  at 30 mK, which shows how the Fano line shape is affected by the magnetic field threading the ring. Note the large AB oscillation of the same order as the resonance peak, indicating that the transport through the system occurs almost coherently. (B) The conductance of several Fano peaks as a function of  $V_g$  and  $B$  at 30 mK. AB oscillation exists even at the midpoint of the resonances. The white line represents the AB phase as a function of  $V_g$ . Note that the AB phase changes by  $2\pi$  through the resonance, and all the resonances are in phase.

Figure 3B shows the result over several Fano resonances in the  $V_g$ - $B$  plane. Clear AB oscillation is observed even at the conductance valley between the resonant peaks. This provides another piece of evidence that the QD in the CB region allows transmission of electrons with the aid of the continuum and that the state in the QD is no longer localized. We plot the conductance maxi-

mum as a function of  $V_g$ , where the phase rapidly but continuously changes by  $2\pi$  across the resonance. Since the measurement was performed in the two-terminal setup that allows only phase changes by multiples of  $\pi$  due to reasons of symmetry, the continuous behavior of the AB phase is unexpected, but may be attributed to the breaking of the time-reversal symmetry [21,22]. Since the AB phase changes only slightly at the conductance valley, all the adjacent Fano resonances are in phase, indicating that the resonance peaks are correlated to each other [21]. Several theoretical prediction on the behavior of the AB phase in the Fano system have been reported [15–17], while they do not seem to perfectly explain the overall behavior discussed above. It is also very different from the results obtained for a normal QD [10] and a Kondo QD [12] in previous two-terminal experiments. This is an important experimental indication that the Fano effect plays a crucial role in the phase evolution of electrons through such a quantum system similar to ours when the coherence is highly preserved [17,23,24].

In the present study, we have clarified a peculiar quantum transport through the QD-AB-ring hybrid system, which is caused by the Fano effect due to the sufficiently coherent transport through the QD and the ring. While this effect has been observed in a variety of physical systems such as in spectroscopy, the present system is the first convincing realization of a tunable Fano system. Controlling of the Fano line shape by the magnetic field has revealed that the Fano parameter  $q$  will be extended to a complex number. The behavior of the AB phase is found to be very different from the previous results, indicating that our system is not simply a QD with an adjective reference arm but should be regarded as a novel quantum system.

This work is supported by a Grant-in-Aid for Scientific Research and by a Grant-in-Aid for COE Research (“Quantum Dot and Its Application”) from the Ministry of Education, Culture, Sports, Science, and Technology of Japan.

and N. S. Wingreen, *Science* **280**, 567 (1998).

- [8] J. Li, W. D. Schneider, R. Berndt and B. Delley, *Phys. Rev. Lett.* **80**, 2893 (1998).
- [9] J. Göres *et al.*, *Phys. Rev. B* **62**, 2188 (2000).
- [10] A. Yacoby, M. Heiblum, D. Mahalu and H. Shtrikman, *Phys. Rev. Lett.* **74**, 4047 (1995).
- [11] R. Schuster *et al.*, *Nature* **385**, 417 (1997).
- [12] W. G. van der Wiel *et al.*, *Science* **289**, 2105 (2000).
- [13] Y. Ji *et al.*, *Science* **290**, 779 (2000).
- [14] M. Kastner, *Phys. Today* **46**, 24 (1993).
- [15] C. M. Ryu and S. Y. Cho, *Phys. Rev. B* **58**, 3572 (1998).
- [16] K. Kang, *Phys. Rev. B* **59**, 4608 (1999).
- [17] O. Entin-Wohlman, A. Aharonov, A., Y. Imry and Y. Levinson, cond-mat/0109328 (2001).
- [18] D. Goldhaber-Gordon *et al.*, *Nature* **391**, 156 (1998).
- [19] S. M. Cronenwett, T. H. Oosterkamp and L. P. Kouwenhoven, *Science* **281**, 540 (1998).
- [20] J. Schmid, J. Weis, K. Eberl and K. von Klitzing, *Physica B* **256–258**, 182 (1998).
- [21] H.-W. Lee, *Phys. Rev. Lett.* **82**, 2358 (1999).
- [22] A. van Oudenaarden, M. H. Devoret, Y. V. Nazarov and J. E. Mooij, *Nature* **391**, 768 (1998).
- [23] B. R. Bulka and P. Stefanski, *Phys. Rev. Lett.* **86**, 5128 (2001).
- [24] W. Hofstetter, J. Konig and H. Schoeller, *Phys. Rev. Lett.* **87**, 156803 (2001).

---

- [1] U. Fano, *Phys. Rev.* **124**, 1866 (1961).
- [2] R. K. Adair, C. K. Bockelman and R. E. Peterson, *Phys. Rev.* **76**, 308 (1949).
- [3] U. Fano and A. R. P. Rau, in *Atomic Collisions and Spectra* (Academic Press, Orlando, 1986).
- [4] F. Cerdeira, T. A. Fjeldly and M. Cardona, *Phys. Rev. B* **8**, 4734 (1973).
- [5] J. Faist, F. Capasso, C. Sirtori, K. W. West and L. N. Pfeiffer, *Nature* **390**, 589 (1997).
- [6] G. D. Mahan, *Many-Particle Physics* (Plenum Press, New York, 1990).
- [7] V. Madhavan, W. Chen, T. Jamneala, M. F. Crommie